JOURNAL OF VIROLOGY, Nov. 2009, p. 11635–11644 Vol. 83, No. 22
0022-538X/09/$12.00 doi:10.1128/JVI.01483-09

General and Target-Specific RNA Binding Properties of Epstein-Barr Virus SM Posttranscriptional Regulatory Protein▽

Zhao Han,[1] Dinesh Verma,[1] Chelsey Hilscher,[2] Dirk P. Dittmer,[2] and Sankar Swaminathan[1]*

Division of Infectious Diseases, Department of Medicine, and University of Florida Shands Cancer Center, University of Florida, Gainesville, Florida,[1] and Department of Microbiology and Immunology, Center for AIDS Research, and Lineberger Comprehensive Cancer Center, University of North Carolina at Chapel Hill, Chapel Hill, North Carolina[2]

Received 16 July 2009/Accepted 24 August 2009

Epstein-Barr virus (EBV) SM protein is an essential nuclear shuttling protein expressed by EBV early during the lytic phase of replication. SM acts to increase EBV lytic gene expression by binding EBV mRNAs and enhancing accumulation of the majority of EBV lytic cycle mRNAs. SM increases target mRNA stability and nuclear export, in addition to modulating RNA splicing. SM and its homologs in other herpesvirus have been hypothesized to function in part by binding viral RNAs and recruiting cellular export factors. Although activation of gene expression by SM is gene specific, it is unknown whether SM binds to mRNA in a specific manner or whether its RNA binding is target independent. SM-mRNA complexes were isolated from EBV-infected B-lymphocyte cell lines induced to permit lytic EBV replication, and a quantitative measurement of mRNAs corresponding to all known EBV open reading frames was performed by real-time quantitative reverse transcription-PCR. The results showed that although SM has broad RNA binding properties, there is a clear hierarchy of affinities among EBV mRNAs with respect to SM complex formation. In vitro binding assays with two of the most highly SM-associated transcripts suggested that SM binds preferentially to specific sequences or structures present in noncoding regions of some EBV mRNAs. Furthermore, the presence of these sequences conferred responsiveness to SM. These data are consistent with a mechanism of action similar to that of hnRNPs, which exert sequence-specific effects on gene expression despite having multiple degenerate consensus binding sites common to a large number of RNAs.

Epstein-Barr virus (EBV) SM is an RNA binding protein that is essential for lytic EBV replication (1, 5, 6, 8, 14, 15, 17, 33–35, 42). The SM gene is homologous to immediate-early or early genes expressed by several other human and animal herpesviruses, including those encoding herpes simplex virus type 1 (HSV-1) ICP27, human cytomegalovirus (HCMV) UL69, varicella-zoster virus open reading frame 4 (ORF4) protein, and Kaposi's sarcoma-associated herpesvirus (KSHV) ORF57 protein/Mta (2, 24, 27, 30, 36, 47). These proteins are multifunctional and function as transcriptional and posttranscriptional regulators of gene expression. One of the major roles of SM is to enhance EBV gene expression by increasing the accumulation of lytic EBV transcripts (5, 21, 39). In experiments performed with cells infected with recombinant EBV with SM deleted, exogenous expression of SM increased the expression of more than 50% of lytic EBV transcripts (15). Most of these SM-responsive transcripts accumulate poorly in the absence of SM. The dependence of these mRNAs on SM is multifactorial, as lytic EBV DNA replication also requires SM, primarily due to SM-enhanced expression of EBV DNA polymerase and primase proteins (15). Thus, SM may stimulate lytic EBV gene expression indirectly, by enhancing lytic EBV replication, as well as by having direct effects on target mRNAs. SM is thought to bind to EBV mRNAs in the nucleus and to enhance mRNA export by recruiting cellular export factors (3, 7, 18). In addition, SM enhances the nuclear accumulation of target mRNAs, suggesting that SM also increases RNA stability (28, 35). SM binds to mRNA targets in vivo, which can be coimmunoprecipitated with SM (33). SM can be UV cross-linked to RNA in vitro, and direct contact of SM with RNA is suggested by transfer of radioactive label from RNA to SM protein (46). An arginine-rich motif in SM has been shown to bind RNA in vitro, and SM mutants with this motif deleted are defective in RNA binding (17).

SM exhibits some degree of preferential cross-linking to RNA targets in vitro, and several lines of evidence indicate that SM exerts gene-specific effects. In reporter assays, SM is particularly active against certain targets, such as chloramphenicol acetyltransferase (33, 35). In addition, as noted above, SM is required for the expression of approximately 60% of EBV lytic genes, but the remainder of EBV lytic genes are expressed efficiently in the absence of SM (15). Further, SM acts as an alternative splicing factor, directing donor splice site usage to a specific alternate 5′ splice site (46). While these findings suggest that SM may preferentially associate with sequence- or structure-based elements present in some mRNAs, it is also possible that SM binds mRNAs nonspecifically but has different effects on various targets. For example, it is possible that some EBV mRNAs possess constitutive transport elements that utilize cellular nuclear export pathways, rendering SM superfluous. Similarly, other mRNAs may be unstable and require SM to bind and stabilize them or protect them from degradation in order to accumulate efficiently. Thus, regardless of the mechanism of action of SM, it is possible that transcript-specific effects of SM may be unrelated to transcript-

* Corresponding author. Mailing address: 1376 Mowry Road, Gainesville, FL 32610-3633. Phone: (352) 273-8206. Fax: (352) 273-8299. E-mail: sswamina@ufl.edu.

▽ Published ahead of print on 2 September 2009.

specific binding. In fact, previous experiments have shown that mRNAs transcribed from both SM-responsive and non-SM-responsive transfected genes are immunoprecipitated equally well with SM (33).

Currently, it is unclear whether SM or its homologs in other herpesviruses associate preferentially with specific transcripts in vivo. In this study, we performed SM immunoprecipitations (IPs) from EBV-infected B lymphocytes and analyzed the RNA in the immunoprecipitates with a quantitative reverse transcription (RT)-PCR (qRT-PCR) microarray. These experiments demonstrated that SM associates preferentially with specific EBV mRNAs and that SM binds to specific portions of these mRNAs in vitro.

MATERIALS AND METHODS

Plasmids and cell lines. EBV BFRF3 DNA from the 5′ untranslated region (UTR) to the cleavage and polyadenylation signal and antisense BFRF3 were cloned by high-fidelity PCR amplification of B95-8 DNA using AccuPrime *Pfx* DNA Polymerase (Invitrogen). The BFRF3 clone included nucleotides from B95-8 EBV genome positions 49056 to 49806 (accession number NC00705) using primers flanking the entire BFRF3 gene, including the 5′ and 3′ UTRs. Restriction sites were incorporated into the PCR primers, and PCR products were directionally cloned into the HindIII and EcoRV sites of pcDNA3 (Invitrogen). The orientations of the inserts were determined by restriction enzyme digestion and confirmed by DNA sequencing.

Subclones of BFRF3, each encompassing approximately one-fourth of the gene extending from the 5′ UTR to 20 nucleotides (nt) downstream of the cleavage and polyadenylation signal of BFRF3, were also constructed by PCR amplification. PCR was performed using specific 5′ and 3′ primers. The PCR products ranged between 186 and 196 nt in length. Each cloned PCR product was screened by restriction digestion and confirmed by DNA sequencing.

The PCR primers were as follows: BFRF3 5′ Q1HindIII, 5′-CTGAAAGC TTTATTTAACTTTGCGGACAGAGG-3′ (nt 49056 to 49078); BFRF3 3′ Q1EcoRV, 5′-TCAGGATATCGTTGGGCTTGGGCAGCCGGCGTG3-′ (nt 49223 to 49243); BFRF3 5′ Q2HindIII, 5′-CTGAAAGCTTCAAGCCCACCCTC CAG-3′ (nt 49236 to 49251); BFRF3 3′ Q2EcoRV, 5′-TCAGGATATCGGCACC CCAAAAGTCCTCTGCAC-3′ (nt 49399 to 49421); BFRF3 5′ Q3HindIII, 5′-CT GAAAGCTTTCGGCGCCAACGCGCCATAGACAAG-3′ (nt 49422 to 49446); BFRF3 3′ Q3EcoRV, 5′-TCAGGATATCGATGAAGAAACAGAGGGGGTC-3′ (nt 49596 to 49616); BFRF3 5′ Q4HindIII, 5′-CTGAAAGCTTTCATCTATTAG CAGCCTC-3′ (nt 49612 to 49629); BFRF3 3′ Q4EcoRV, 5′-TCAGGATATCAG TTTTTGTATCTGTAATTG-3′ (nt 49787 to 49806); BFRF3 5′ EcoRV, 5′-TCAG GGATATCTATTTAACTTTGCGGACAGAG-3′ (nt 49056 to 49077); BFRF3 3′ HindIII, 5′-CTGAAAGCTTAGTTTTTGTATCTGTAATTG-3′ (nt 49787 to 49806); BDLF3 5′ Q1 HindIII, 5′-CTGAAAGCTTTATAAAAGAGGCCGGGA G-3′ (nt 118816 to 118799); BDLF3 3′ Q1 EcoRV, 5′-TCAGGATATCGATGCC GACGGTGATGG-3′ (nt 118990 to 119006); BDLF3 5′ Q2 HindIII, 5′-CTGAA AGCTTGGGTCCTAGCACAAACCAG-3′ (nt 119007 to 119025); BDLF3 3′ Q2 EcoRV, 5′-TCAGGATATCTCCTGTTCCGGCCTCGGTG-3′ (nt 119193 to 119210); BDLF3 5′ Q3 HindIII, 5′-CTGAAAGCTTAACCTCCACGGGTGTGA CTAG-3′ (nt 119211 to 119231); BDLF3 3′ Q3 EcoRV, 5′-TCAGGATATCCCA GAGAGGAAGACCGTAAG-3′ (nt 119390 to 119409); BDLF3 5′ Q4 HindIII, 5′-CTGAAAGCTTACACTGGTGTTTGTGGGGC-3′ (nt 119410 to 119428); and BDLF3 3′ Q4 EcoRV, 5′-TCAGGATATCTTCAAGAAAGTTCATTAAAC-3′ (nt 119568 to 119587).

Cell lines. P3HR1 is a Burkitt lymphoma cell line infected with EBV type 2 (31), and B95-8 is a marmoset B-cell line transformed by EBV type 1 (26). Both cell lines were transfected and selected to stably express a fusion protein containing the BZLF1 transactivator of early lytic cycle replication fused to the hormone domain of the estrogen receptor, which, in the presence of 4-hydroxytamoxifen (4-HT), allows the functional release of BZLF1, inducing lytic EBV replication (19, 45). The P3HR1-ZHT and B958-ZHT cell lines were propagated in RPMI supplemented with 10% fetal bovine serum (HyCLone), 0.8 mg/ml G418 (AG Scientific), and GlutaMax (Invitrogen). Cos7 cells are African green monkey kidney fibroblast cells transformed with a mutant simian virus 40 (13). These cells were maintained in Dulbecco's modified Eagle medium supplemented with 10% fetal bovine serum and L-glutamine. All cells were grown at 37°C in 5% CO_2.

IP and RNA isolation. Lytic replication was induced in 1.8×10^7 P3HR1-ZHT or B958-ZHT cells at 5×10^5 cells/ml by adding 100 nM 4-HT to the cell growth medium. Cells were harvested 48 h after the addition of 4-HT and lysed in ice-cold IP lysis buffer (Tris-buffered saline [pH 7.4], 1% Triton X-100, and protease inhibitor cocktail; Sigma-Aldrich) prepared with RNase-free reagents. All subsequent steps were performed at 4°C. The cells were incubated in lysis buffer for 10 min on ice with frequent mixing and were sonicated to ensure maximum lysis. The lysed-cell suspension was centrifuged for 10 min at $10^5 \times g$. The supernatant was transferred to fresh tubes and precleared by incubation with 0.8 μg of normal rabbit immunoglobulin G (Bethyl) per 10^6 cells, followed by incubation with protein A-conjugated agarose beads (Sigma) for 2 h. The cleared supernatants were then immunoprecipitated with either preimmune (PI) serum or rabbit polyclonal anti-SM antibody (0.8 μg antibody per 10^6 cells) overnight, followed by incubation with protein A-agarose beads for 2 h. The beads were washed four times in IP wash buffer (500 mM NaCl, 25 mM Tris, 27 mM KCl, 1% NP-40 [pH 7.4]). Coimmunoprecipitated RNA was isolated from the immunoprecipitates using RNA-bee (Teltest), Glycoblue (Ambion), and RNeasy columns (Qiagen) with an on-column DNase treatment (Qiagen) and eluted with RNase-free Tris-EDTA buffer. RNA was quantitated by spectrophotometry.

cDNA microarray and analysis. Real-time qRT-PCR arrays containing PCR primers targeting all ORFs of the EBV genome were designed and performed as previously described (23). RNA used in the microarray analysis was coimmunoprecipitated and purified as described above. RT of RNA was performed with reverse transcriptase (Invitrogen), 2 mM deoxyribonucleoside triphosphates, 2.5 mM $MgCl_2$, RNAsin (Applied Biosystems Inc.), and random hexamers. The conditions for RT were 42°C for 45 min, 52°C for 30 min, and 70°C for 10 min. Following RT, the removal of excess RNA was performed by incubation of each RT reaction mixture with 1 U of RNase H at 37°C. Real-time PCR was performed in triplicate for each sample with SYBR green PCR mix (Applied Biosystems) using universal cycling conditions (29). Raw cycle threshold (C_T) values were determined by threshold analysis and used directly to compare differences.

Northern blotting. P3HR1-ZHT and B958-ZHT cells were induced to permit lytic replication by incubating the cells at 5×10^5 cells/ml in 100 nM 4-HT; 10^7 cells were harvested for RNA at 0 and 48 h after induction, and RNA coimmunoprecipitated with SM was isolated as described above. RNA samples were electrophoresed in a 1% denaturing formaldehyde agarose gel, transferred to a nylon membrane (Zeta Probe; Bio-Rad), and UV cross-linked to the membrane. Gene-specific probes were generated by PCR amplification, gel purification, and random-primer labeling with [α-^{32}P]dCTP. The probes were hybridized to blots overnight at 65°C, washed, and exposed to film and a phosphorimager screen for quantification by ImageQuant software (GE Healthcare).

In vitro photo-cross-linking and RNA label transfer assay. Cos7 cells were transfected with empty-vector plasmid (pcDNA3; Invitrogen) or SM expression vector DNA (35) using Lipofectamine Plus (Invitrogen) in 100-mm dishes with 6 μg of DNA per transfection dish, according to the manufacturer's protocol. The cells were harvested 48 h after transfection. The cells were washed with warm Dulbecco's modified Eagle's medium-10% fetal bovine serum, gently scraped off, and pelleted by centrifugation at 20°C for 5 min at $900 \times g$. The cells were lysed by resuspending the pellets in twice the pellet volume of ice-cold lysis buffer (20 mM HEPES [pH 7.9], 10 mM NaCl, 10% glycerol, 3 mM $MgCl_2$, 0.1% NP-40, 0.2 mM EDTA, 0.4 mM phenylmethylsulfonyl fluoride, 1 mM dithiothreitol, and eukaryotic protease inhibitor cocktail σ) and incubating the suspension at 4°C for 15 min with frequent gentle mixing. The lysed-cell suspensions were centrifuged at 4°C for 5 min at $15{,}000 \times g$. The cleared supernatants were transferred to a fresh tube, and high-salt buffer (20 mM HEPES [pH 7.9], 400 mM KCl, 20% glycerol, 0.2 mM EDTA, 0.4 mM phenylmethlysulfonyl fluoride, 1 mM dithiothreitol, and protease inhibitor cocktail σ) was added at one-third the volume of the supernatant. Aliquots of protein extracts were snap-frozen and stored at −80°C.

RNAs were synthesized using full-length BFRF3, BFRF3 subclones, or antisense BFRF3 plasmid DNAs, previously linearized with EcoRV, in the presence of [α-^{32}P]rUTP (Perkin Elmer) and T7 RNA polymerase (NEB). Radioactively labeled RNA transcripts were separated on denaturing urea-polyacrylamide gels, and full-length transcripts were excised. Gel slices were crushed in a microcentrifuge tube, and RNA was eluted by incubation in 0.5 M NH_4 acetate, 10 mM Mg acetate, 0.1 mM EDTA, 0.1% sodium dodecyl sulfate (SDS) for 10 min at 65°C. The eluate was filtered twice and ethanol precipitated, and RNA was resuspended in double-distilled H_2O. The integrity of the purified labeled RNA was verified by polyacrylamide gel electrophoresis (PAGE) and autoradiography, and the radioactivity was quantitated by Cerenkov counting. UV cross-linking was performed by incubating 2×10^6 cpm of each purified radiolabeled RNA with 8 μl of cell extract, 2 μl of 20 mM magnesium acetate, 2 μl of 10 mM ATP,

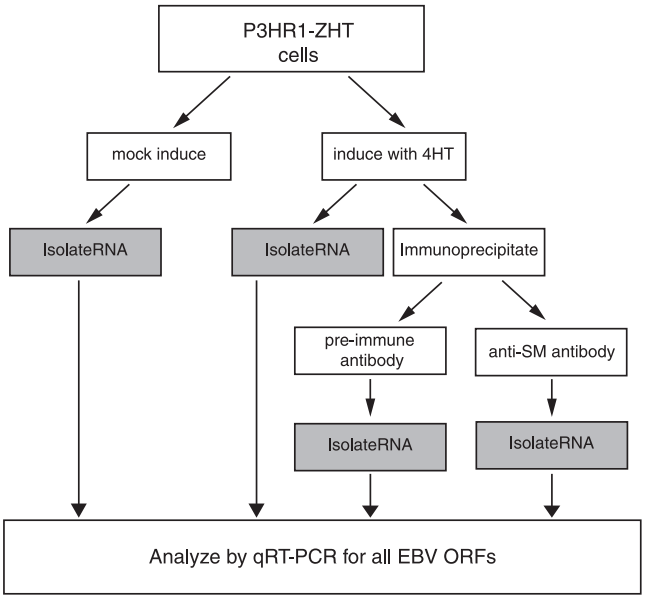

FIG. 1. Experimental design for quantitative analysis of RNA association with SM in EBV-infected cells. Lymphoma cells were either mock induced or induced to permit lytic EBV replication, and the cells were divided into fractions for immediate RNA isolation (gray boxes) or IP. After IP with either control or SM-specific antibody, RNA was isolated from the immunoprecipitates. All RNA was reverse transcribed, and the relative amount of each EBV transcript was measured by qRT-PCR.

2 μl of 200 mM potassium glutamate, 2 μl of 50 mM creatine phosphate, 1 μl of tRNA (1 mg/ml), and 1 μl of RNAsin (Promega) in a total volume of 20 μl. The reaction mixtures were incubated at 30°C for 30 min in the lid of a microcentrifuge tube, and RNA-protein complexes were UV cross-linked on ice in a Stratalinker (Stratagene) by exposure to 0.6 J/cm^2. Samples were digested with RNase A at 100 μg/ml for 1 h at 37°C and immunoprecipitated using anti-SM antibody and protein A-agarose beads. Purified proteins were separated on 10% SDS-PAGE gels, followed by exposure on a phosphorimager screen and film.

RESULTS

Analysis of RNA isolated from SM immunoprecipitates from Burkitt lymphoma cells revealed a hierarchy of RNA affinities with SM. The presence of mRNA in association with SM in immunoprecipitates from SM-transfected cells was previously demonstrated (33). Only three target transcripts were measured, and no differences in binding to SM were observed, although SM appeared to associate preferentially with newly transcribed mRNA. The RNA in those studies was detected by a sensitive RNase protection assay, and it was unclear whether IP of SM from EBV-infected cells would yield associated RNA in amounts adequate to be analyzed by qRT-PCR for all EBV transcripts. We therefore utilized a cell line derived from the Burkitt lymphoma cell line, P3HR1, that was engineered to permit efficient, high-level lytic EBV replication and gene expression (45). The P3HR1-ZHT cell line contains a stably transfected chimeric gene consisting of the Z immediate-early transactivator fused to a 4-HT-specific hormone binding domain. These cells efficiently permit the resident EBV to enter the lytic phase of EBV replication when 4-HT is added to the growth medium. The strategy of the experiment is outlined in Fig. 1. P3HR1-ZHT cells were induced or mock induced with 4-HT to permit EBV lytic replication and harvested 48 h after induction. One fraction of the cells was immediately processed to isolate total cellular RNA by lysis of the cell pellet in a guanidinium isothiocyanate-phenol solution (RNA-Bee). The remainder of the cells were lysed with detergent, in the presence of both protease and RNase inhibitors and immediately divided into two aliquots, which were immunoprecipitated with either anti-SM antibody or PI antibody. The immunoprecipitates were then processed for isolation of any associated RNA after the addition of dye-labeled glycogen as a carrier. These RNAs were then analyzed by qRT-PCR using primers specific for all known EBV ORFs. These analyses essentially provided us with four quantitative measurements for each EBV mRNA: (i) its abundance before induction of lytic replication, (ii) its abundance 48 h after induction, (iii) its relative abundance in SM immunoprecipitates 48 h after induction, and (iv) its relative abundance in control IPs performed with PI serum. These measurements therefore allowed, for each mRNA, determination of its level of induction during lytic replication, its abundance relative to all EBV transcripts, and its relative abundance in association with SM. In addition, the control IP allowed correction for nonspecific IP of mRNA.

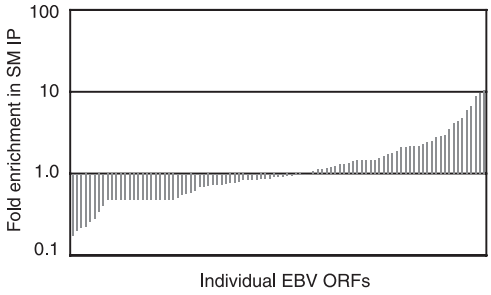

FIG. 2. Relative abundances of EBV mRNAs associated with SM. C_T values from qRT-PCR for each EBV transcript in the RNA isolated from the SM IP were converted to the increase above or below the mean enrichment for all transcripts (y axis). Enrichment for each transcript was determined by comparison of its C_T value in the SM IP versus its C_T value in the control immunoprecipitate. Each EBV mRNA is represented by a bar on the x axis, and its enrichment relative to the mean amount of all RNAs is represented on the y axis.

Raw C_T values representing the relative abundances of transcripts immunoprecipitated with SM versus those in the control immunoprecipitates were determined. The amount of RNA in the SM IP was compared to that in the PI IP for each ORF, and the relative enrichment by SM for each RNA target was determined. There was a general enrichment for RNA in the SM IP versus the control (PI IP), demonstrating that SM bound significantly more RNA than the control. In induced P3HR1-ZHT cells, approximately seven times more RNA was immunoprecipitated by SM than in the control IP. This verified the documented RNA binding activity of SM.

Using a linear regression model and the raw C_T values for the mRNA in SM IPs and PI IPs, a mean enrichment for all EBV mRNAs in the SM IPs was calculated. This allowed a ranking of all EBV mRNAs in terms of relative enrichment in the SM IP (Fig. 2). The graph in Fig. 2 reveals the wide range of affinities for SM, resulting in amounts of individual mRNAs in the SM IP from 10-fold to 0.1-fold of the mean amount. These findings therefore indicate that binding of individual

TABLE 1. EBV transcripts highly enriched in SM immunoprecipitates from P3HR1-ZHT cells[a]

Gene	Sample C_T PI	Sample C_T SM	ΔC_T	Enrichment over mean (C_T)	Fold enrichment over mean
BFRF3	29.79	24.15	5.64	3.4	10.6
BGLF5	32.05	26.78	5.27	3.3	9.8
BDLF3	34.51	29.67	4.84	3.1	8.6
BTRF1	32.84	28.20	4.64	2.7	6.5
BCRF1	36.88	32.87	4.01	2.6	6.1
BBRF3	27.79	23.04	4.75	2.3	4.9
BBRF2	36.58	33.05	3.53	2.1	4.3
BALF2	29.10	27.69	1.41	-0.8	0.6

[a] The C_T values from qRT-PCR of RNAs isolated from control IPs and SM IPs and the ΔC_T are shown for the transcripts most highly overrepresented in the SM IP. The values for BALF2, a transcript that was underrepresented in the SM IP, are also shown for comparison. Enrichment in the SM IP relative to the mean enrichment for all mRNAs in the IP is shown as C_T and as enrichment.

EBV mRNAs is highly transcript dependent. Table 1 lists the most highly SM-associated mRNAs, such as BFRF3, which was 10.6-fold more abundant than the mean, translating into 100-fold greater abundance in the SM IP than the least abundant mRNAs. The functions of the genes encoding the most highly SM-associated mRNAs and their temporal classes are shown in Table 2. There was no clear correlation between the temporal class of the gene and association of its transcript with SM, as both early and late lytic transcripts were enriched in SM IPs. This outcome was not unexpected, since a time point after induction at which most EBV mRNAs were actively transcribed and the cells were still viable was chosen for harvest.

Affinity for SM does not correlate with transcript abundance or level of induction. The level of transcript abundance at 48 h after the induction of lytic replication varied considerably among the 80 genes measured. Raw C_T values for the various transcripts varied by as much as 20 cycles (Fig. 3A). Since almost all transcripts were enriched in the SM IP, albeit to varying degrees, it was possible that SM bound mRNA nonspecifically and that greater association with SM was merely a function of transcript abundance. However, as shown in Fig. 3B, the level of each transcript measured by qRT-PCR in the total RNA from induced cells did not correlate with whether a particular transcript was enriched in the SM IP, demonstrating that relative association with SM is not merely a function of the absolute amount of transcript present. This finding is a critical aspect of the interpretation of the binding

TABLE 2. Gene functions and classifications of SM-associated transcripts

Gene	Function	Type
BFRF3	Viral capsid antigen	Late
BGLF5	Host shutoff; alkaline exonuclease	Early
BDLF3	Glycoprotein	Late
BTRF1	Probable tegument protein	Late
BCRF1	viral interleukin 10	Late
BBRF3	Glycoprotein M homolog	Late
BBRF2	Viral tegument protein	Late
BDLF2	Envelope glycoprotein	Late
BNLF2b	Unknown	Early
BALF2	Single-stranded DNA binding protein	Early

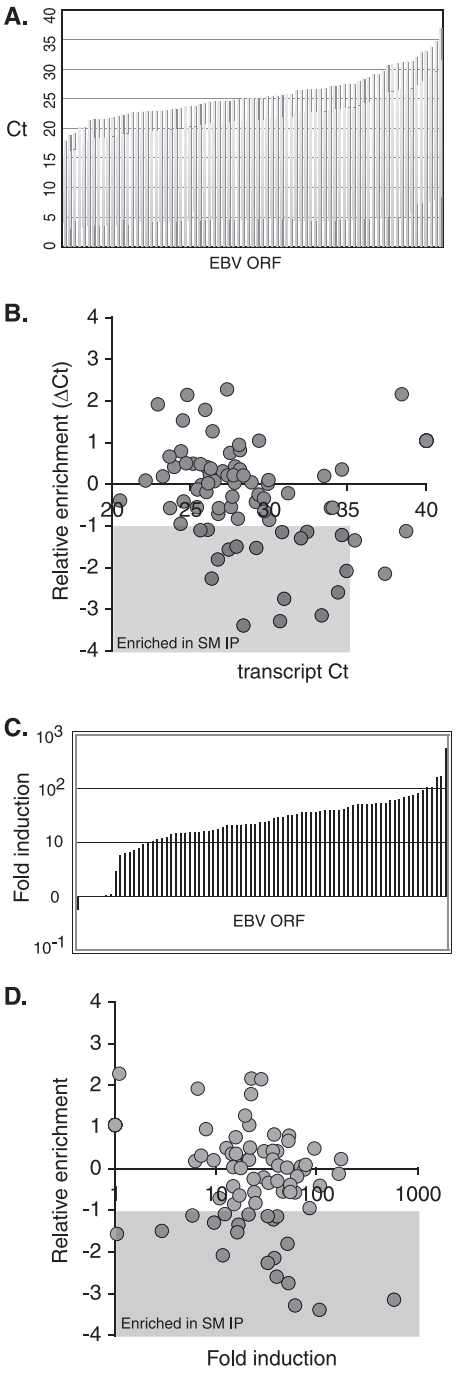

FIG. 3. Relationship of SM association to transcript abundance and level of gene induction. (A) The C_T value for each EBV transcript in the total RNA from induced P3HR1-ZHT cells is shown on the *y* axis, with each EBV transcript plotted on the *x* axis, demonstrating the range and distribution of transcript abundances. (B) Scatter plot of the relative enrichment of each transcript in the SM IP relative to the mean enrichment for all transcripts (ΔC_T; *y* axis) versus the abundance of each transcript (C_T; *x* axis). The area highlighted in gray contains those transcripts highly enriched in the SM IP. (C) The level of induction of each EBV transcript during lytic replication (ΔC_T in induced versus uninduced P3HR1-ZHT RNA) is represented on a logarithmic *y* axis, and each EBV transcript is plotted on the *x* axis. (D) Scatter plot of the relative enrichment of each transcript in the SM IP versus the control IP (ΔC_T; *y* axis) versus the level of induction of each transcript on a logarithmic *x* axis.

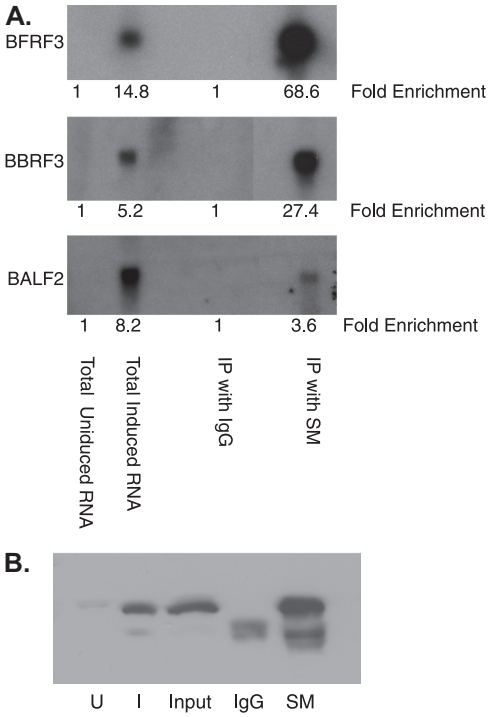

FIG. 4. Northern blot analysis of SM-enriched and unenriched EBV RNAs. (A) RNA from mock-induced P3HR1-ZHT cells, induced cells, PI IP, and SM IP were analyzed by Northern blotting for BFRF3 and BBRF3 (identified as SM associated by qRT-PCR) or BALF2 (non-SM enriched). The relative amounts of RNA were quantitated by phosphorimager measurement and are shown below the lanes. IgG, immunoglobulin G. (B) The amounts of SM present in the total cell lysate from uninduced (U) and induced (I) P3HR1-ZHT cells, input lysate (Input), the control IP (IgG), and SM IP (SM) were measured by immunoblotting with anti-SM antibody; 1% of input lysate and 15% of the IP from cells are shown.

data, since one would expect a correlation between the total amount of each mRNA and the amount found in the SM IP if SM was binding to all mRNAs nonspecifically.

As we have previously shown, SM may associate with nascent transcripts (33), and therefore, the relative level of induction of a transcript may also play a role in how likely it is to be associated with SM at a given time. The level of induction of each transcript during lytic replication varied considerably among the genes measured, ranging from zero to several hundredfold (Fig. 3C). It was therefore relevant to assess whether association with SM was more likely among highly induced transcripts. This analysis demonstrated that the level of induction was not correlated with preferential association with SM, suggesting that such association derives from sequence- or structure-related properties intrinsic to the transcripts (Fig. 3D).

In order to confirm the qRT-PCR findings, Northern blotting of representative transcripts from both the total-RNA and SM IPs was performed (Fig. 4). BFRF3, BBRF3 (highly SM associated), and BALF2 (not highly SM associated) were chosen for further analysis. BFRF3 is the small EBV capsid antigen, BBRF3 is the EBV glycoprotein M homolog, and BALF2 is the single-stranded DNA binding protein. When the level of expression was measured at 0 h and 48 h after the induction of lytic replication, these genes were induced 15-, 5-, and 8-fold, respectively. The level of each transcript in the SM IPs was enriched approximately 70-, 27-, and 4-fold over the amounts found in the control IP. The level of enrichment detected in the SM IPs by Northern blotting therefore correlated well with the amounts measured with the qRT-PCR array (approximately 75-, 35-, and 4-fold enrichment in the SM IPs) and confirmed the differences in transcript affinity for SM measured by qRT-PCR.

Preferential association with SM of EBV transcripts from B95-8 cells. Examination of SM binding to EBV transcripts was also performed in B95-8 cells that had been stably transfected with the Z-HT construct, permitting high-level lytic replication. In fact, lytic replication was extremely robust in these cells, exceeding that observed in P3HR1-ZHT cells, with visible lysis of the majority of cells by 72 to 96 h after induction of lytic replication. The relative association of all EBV transcripts with SM was measured as it was with P3HR1-ZHT cells. Lysates from B95-8-ZHT cells harvested 48 h after induction were immunoprecipitated with anti-SM or PI serum and analyzed by qRT-PCR. The total amount of EBV RNAs isolated in the B95-8 SM IPs was much greater than that observed in P3HR1 cells and approximately 55 times greater than that in the control IPs. This difference may reflect higher expression of lytic genes in B95-8-ZHT cells. Nevertheless, a hierarchy of association with SM was again observed among the various EBV transcripts (Fig. 5 and Table 3). The enrichment was as much as 37-fold over the mean enrichment, which, as noted, was already 55-fold, whereas some transcripts, such as BALF2, did not appear to associate significantly with SM and were present at levels far below the mean enrichment. Of the seven B95-8 transcripts most highly associated with SM, five were also among the most highly SM-associated P3HR1 mRNAs, again suggesting that transcript-specific properties determine affinity for SM in vivo. These five transcripts were BFRF3, BDLF3, BBRF3, BBRF2, and BTRF1 (Tables 2 and 3).

A comparison of the absolute levels of B95-8 transcripts with the likelihood of association with SM in the SM immunoprecipitate was performed (Fig. 5B). Transcripts whose absolute C_T levels in the qRT-PCR measurement varied by as much as 5 C_T units (approximately 30-fold difference) were highly represented in the SM IPs. Thus, the results again indicated that preferential association with SM was not simply due to the greater abundance of some transcripts.

The qRT-PCR array results were verified for representative genes by Northern blotting, as was done with P3HR1-ZHT lysates (Fig. 5C). The three genes BFRF3, BBRF3 (highly SM-associated), and BALF2 (less SM associated) were present in the total induced RNA population at similar levels (8- to 15-fold over uninduced) but were immunoprecipitated by SM at significantly different levels (3.5-fold in the case of BALF2 versus 38- and 60-fold over control IPs in the cases of BBRF3 and BFRF3).

SM exhibits sequence-specific binding to EBV transcripts in vitro. The finding that SM associated preferentially with certain EBV transcripts led us to ask whether SM bound more avidly to specific sites within such transcripts. RNA binding proteins that bind RNA directly can be shown to contact RNA using a UV cross-linking and label transfer assay. We had previously shown that SM in cell lysates could be labeled by incubation and UV cross-linking to [^{32}P]rUTP-labeled RNA

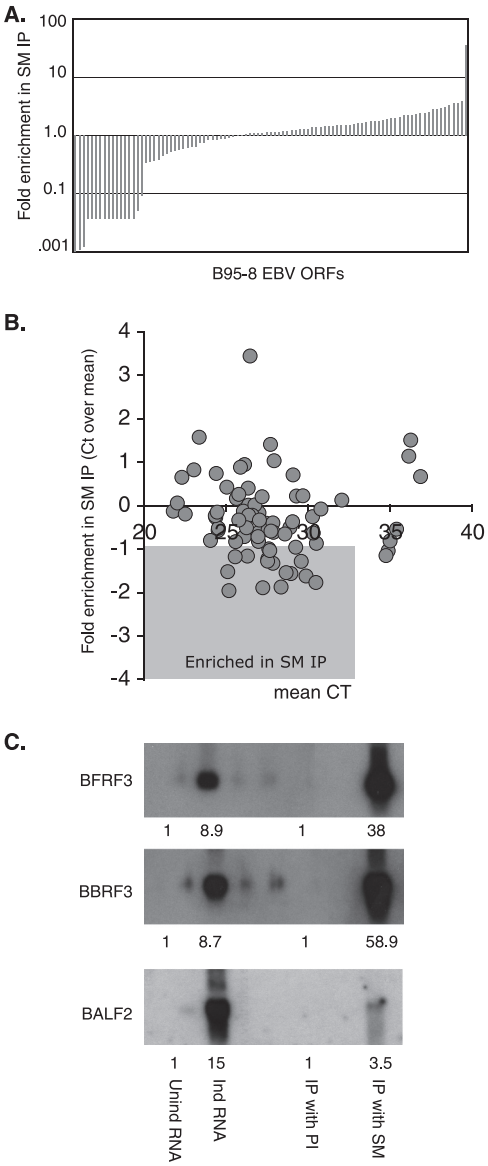

FIG. 5. EBV RNAs associated with SM in B95-8 cells. (A) Enrichment of each EBV transcript (the amount in SM IP versus PI IP) compared to the mean enrichment for all transcripts in the SM IP was calculated and plotted on the logarithmic *y* axis. Each EBV mRNA is represented by a bar on the *x* axis. (B) Scatter plot of the relative enrichment of each transcript in the SM IP versus the mean enrichment for all transcripts (ΔC_T; *y* axis) versus the abundance of each transcript (C_T; *x* axis). The area highlighted in gray contains those transcripts most highly enriched in the SM IP. (C) RNAs from mock-induced B95-8ZHT cells, induced cells, PI IP, and SM IP were analyzed by Northern blotting for BFRF3 and BBRF3 (identified as SM associated by qRT-PCR) or BALF2 (non-SM enriched). The relative amounts of RNA were quantitated by phosphorimager measurement and are shown below the lanes.

transcripts in vitro (46). RNase hydrolysis of non-cross-linked nucleotides and IP of SM, followed by SDS-PAGE and autoradiography, allowed the visualization of labeled SM protein. In order to compare the relative abilities of regions of BFRF3 mRNA to bind SM, in vitro-labeled transcripts corresponding to four segments of the entire BFRF3 gene comprised of 190, 205, 199, and 178 nt spanning the 5′ UTR, coding regions, and 3′ UTR of BFRF3 were generated by transcription with T7 RNA polymerase. In addition, full-length BFRF3 transcript and antisense BFRF3 transcripts were synthesized. The integrity and size of each radiolabeled transcript was verified by polyacrylamide gel electrophoresis, and each transcript was purified by excision and elution from the gel (Fig. 6A). Interestingly, antisense BFRF3 did not cross-link to SM protein, whereas full-length BFRF3 transcript strongly labeled SM protein under identical conditions, suggesting that BFRF3 RNA contains specific sequences or secondary-structure elements that contact SM protein (Fig. 6B). Further, analysis of the four subclones of BFRF3 revealed that the first 190 nt of the transcript, which includes the 5′ UTR, bound most strongly to SM. While there was some binding of the second quarter (Q2) of the BFRF3 transcript, there was virtually no binding by Q3 and Q4 of the BFRF3 transcript (Fig. 6C).

A similar analysis was performed with the BDLF3 transcript, which was identified as strongly SM associated in both P3HR1 and B95-8 cells (Fig. 7A). Full-length BDLF3 transcript exhibited strong binding, whereas the antisense transcript again did not exhibit significant label transfer to SM. In the case of BDLF3, both Q1 and Q4 of the transcript exhibited greater label transfer to SM than did Q2 and Q3 of the BDLF3 transcript. A fainter band that migrated at approximately the same mobility as SM, which was also present in lysates lacking SM (data not shown) and likely represents a cellular RNA binding protein, was also detected in these experiments. Thus, both BDLF3 and BFRF3 transcripts exhibited specific interactions with SM in vitro, and these interactions appeared to map to specific regions of each transcript. A similar analysis was performed to assess the in vitro binding of BALF2 RNA, which did not strongly associate with SM in vivo. As shown in Fig. 7B, BALF2 RNA did not bind appreciably to SM compared to BFRF3 RNA, consistent with the in vivo binding data, in which BALF2 mRNA was not overrepresented in SM immunoprecipitates.

SM binding affinity in vitro and in vivo correlates with enhanced RNA accumulation in response to SM. The findings that sequences in highly SM-associated mRNAs, such as BFRF3 and BDLF3, contained sequences that cross-linked to SM in vitro suggested that these sequences could act as SM

TABLE 3. EBV transcripts highly enriched in SM immunoprecipitates from B95-8-ZHT cells[a]

Gene	Sample C_T PI	Sample C_T SM	ΔC_T	Enrichment over mean (C_T)	Fold enrichment over mean
BDLF3	40	30.04	>9.96	5.23	37.5
BNLF2b	40	30.13	>9.87	5.14	35.3
BBRF3	34.44	27.51	6.93	1.95	3.9
BFRF3	32.66	25.2	7.46	1.88	3.7
BGLF2	33.98	26.69	7.29	1.86	3.6
BTRF1	35.76	28.93	6.83	1.61	3.1
BBRF2	34.44	27.51	6.93	1.55	2.9
BALF2	31.66	30.26	1.4	−4.30	0.05

[a] The C_T values from qRT-PCR of RNAs isolated from control IPs and SM IPs and the ΔC_T are shown for the transcripts most highly overrepresented in the SM IP. The values for BALF2, a transcript that was underrepresented in the SM IP, are also shown for comparison. Enrichment in the SM IP relative to the mean enrichment for all mRNAs in the IP is shown as C_T and as enrichment.

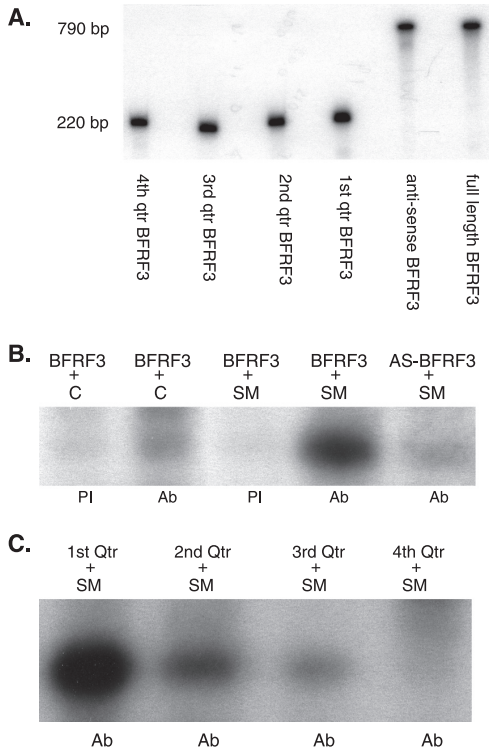

FIG. 6. In vitro binding of SM to BFRF3 RNA. (A) In vitro-transcribed and [^{32}P]UTP-labeled RNA corresponding to four quarters (qtr) of the BFRF3 mRNA, full-length mRNA, and antisense mRNA were purified by urea-PAGE electrophoresis. (B) Radiolabeled BFRF3 transcripts or antisense BFRF3 transcripts (AS-BFRF3) were incubated with lysates from cells transfected with empty vector (C) or SM as shown above each panel and cross-linked with UV light. RNase-treated samples were immunoprecipitated with either PI serum (PI) or anti-SM antibody (Ab), electrophoresed, and analyzed by autoradiography. (C) Transcripts from each quarter of BFRF3 were incubated with SM lysate and analyzed as for panel B.

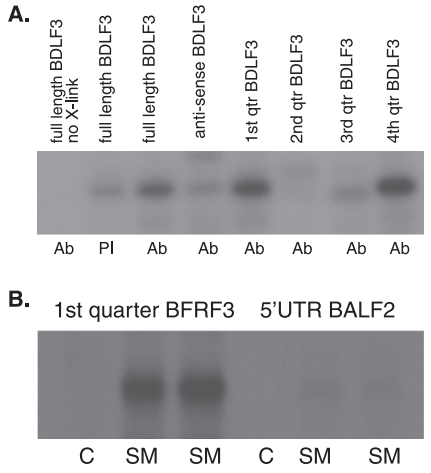

FIG. 7. In vitro binding of SM to BDLF3 RNA. (A) Full-length BDLF3 RNA, antisense BDLF3, or transcripts from four quarters (qtr) of the BDLF3 gene were analyzed for binding to SM by in vitro photo-cross-linking and label transfer assay. A control reaction performed in parallel without UV cross-linking (no X-link) is also shown. (B) Transcripts from Q1 of BFRF3 or the corresponding region of BALF2 were incubated with SM lysate (SM) in duplicate or mock-transfected lysate (C) and analyzed as for panel A.

response elements. In order to ask whether the presence of a sequence with high affinity for SM could confer increased responsiveness to SM on a heterologous mRNA, we tested the effect of fusing different BFRF3 subclones to the 5′ UTR of a reporter gene. The first 190 nt and the last 178 nt of the BFRF3 gene were each fused to the 5′ terminus of the luciferase gene in the pGL3 reporter plasmid. Each construct was transfected in HeLa cells with either empty vector or the SM expression plasmid. Accumulation of luciferase mRNA from each fusion gene in the nucleus and cytoplasm was then measured by Northern blotting. In the presence of SM, the levels of luciferase mRNA fused to BFRF3 Q1 were higher than those of the BFRF3 Q4 fusion, particularly in the cytoplasm (Fig. 8A).

This result indicated that the presence of BFRF3 Q1 sequence that exhibited high affinity for SM in vitro conferred increased accumulation in the presence of SM. One would therefore expect that this RNA would also accumulate to greater levels in the presence of SM than BFRF3 Q4, which bound SM with less affinity in vitro. We therefore transfected either BFRF3 Q1 or BFRF3 Q4 transcribed from a CMV promoter along with SM plasmid or empty vector and compared the accumulation of each corresponding BFRF3 RNA in the presence or absence of SM. As predicted, the BFRF3 Q1 RNA accumulated to significantly higher levels than BFRF3 Q4 RNA when SM was present (Fig. 8B).

In order to determine whether the differences between these two RNA sequences in enhancement by SM correlated with SM association in vivo, as might be expected based on the in vitro cross-linking results, we measured the amounts of BFRF3 Q1 versus BFRF3 Q4 RNA immunoprecipitable with SM. Full-length BFRF3, BFRF3 Q1, or BFRF3 Q4 plasmid was transfected along with SM plasmid, and RNA was isolated from SM immunoprecipitates, as was done from P3HR1-ZHT cells. When the SM-associated RNAs were measured by Northern blotting, it was clear that BFRF3 Q1 was more highly associated with SM. It should be noted that since SM enhances the accumulation of BFRF3 Q1 more than accumulation of BFRF3 Q4, the total amount of BFRF3 Q4 RNA was significantly less than BFRF3 Q1 or full-length BFRF3 RNA. Nevertheless, as can be seen in Fig. 8C, the percentage of BFRF3 Q1 RNA or full-length BFRF3 RNA found in association with SM was greater than that of BFRF3 Q4 RNA. In order to ensure that SM was recovered with equal efficiency in each IP, the amount of SM in each input lysate and each IP was quantitated by immunoblotting (Fig. 8C, bottom).

DISCUSSION

One of the current models for the mechanism of action of SM and its homologs in other herpesviruses, such as HSV-1 ICP27, HCMV UL69, and KSHV ORF57 protein/Mta, postulates that these proteins bind to intronless viral mRNAs and, by binding to one or more cellular nuclear export factors, facilitate the export of viral RNAs (for a review, see reference 38). A central aspect of this model is that SM and its homologs compensate for the lack of export factor recruitment that normally occurs concomitant with splicing of intron-containing genes (22, 32, 48). However, a basic question that is not ad-

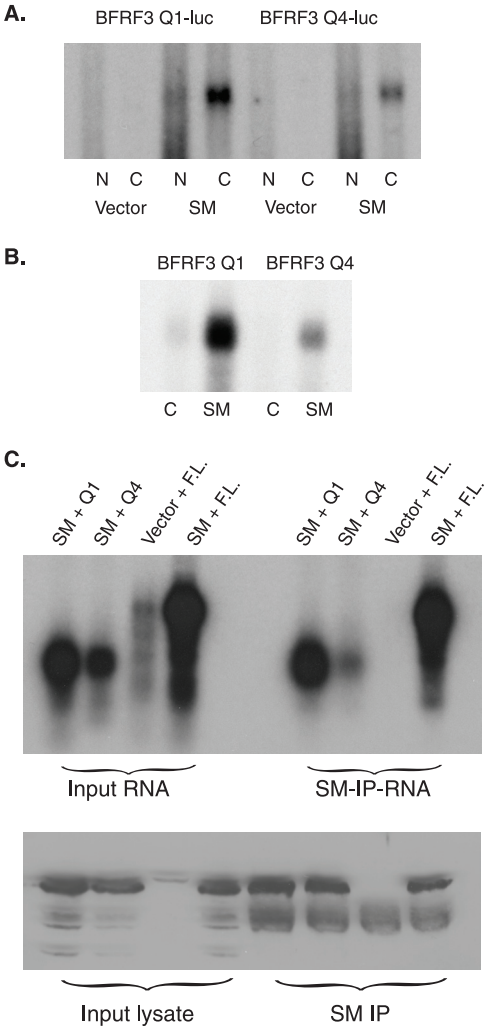

FIG. 8. Differential binding of BFRF3 subclones to SM in vivo and activity as an SM response element. (A) Plasmids in which BFRF3 Q1 or BFRF3 Q4 was fused upstream of the luciferase (luc) coding sequence in a reporter vector were cotransfected with either vector or SM expression plasmid. RNA was isolated from both the nuclei (N) and cytoplasm (C) of transfected cells and analyzed by Northern blotting with luciferase probe. (B) BFRF3 Q1 and BFRF3 Q4 plasmids were transfected with either vector or SM plasmid, and RNA was analyzed by Northern blotting with BFRF3 probe. (C) Cells were transfected with SM and either BFRF3 Q1, BFRF3 Q4, or full-length BFRF3 plasmid (F.L.). RNA was isolated from total cell lysate (input RNA) or from SM immunoprecipitates (SM-IP-RNA) and analyzed by Northern blotting with BFRF3 probe. The amounts of SM in the input lysate and in each immunoprecipitate (SM IP) were measured by immunoblotting and are shown below.

dressed by such models is whether RNA-specific binding occurs and whether it is required for the functions of these proteins.

While much evidence exists for the ability of EBV SM, HSV-1 ICP27, HCMV UL69, and KSHV ORF57/Mta proteins to bind RNA, relatively little is known about the target specificity of these interactions, and the mechanism by which these proteins bind to specific viral RNAs or RNA motifs remains poorly characterized (4, 9, 17, 25, 33, 43). HSV ICP27 has been shown to associate with seven intronless HSV transcripts, but not with two intron-containing HSV transcripts, during lytic HSV infection (37). ICP27 was also shown to associate with 31 HSV RNAs in a yeast three-hybrid assay (41). In this study, the only identified characteristic of RNAs binding to ICP27 was the presence of multiple G nucleotide repeats. Aside from the suggestion that poly(G) sequences may increase ICP27 interaction, which is consistent with a previous study comparing ICP27 binding to poly(G) and poly(U) (25), there was no additional characterization of the relative affinities of various RNAs for ICP27. More recently, systematic evolution of ligands by exponential enrichment has been used to define a potential RNA motif targeted by herpesvirus saimiri ORF57 protein (9). Repetitive selection with oligonucleotide libraries identified GAAGRG as a potential ORF57 protein binding site. The motif was found in multiple herpesvirus saimiri ORFs, and deletion of the motif from a herpesvirus saimiri RNA led to loss of ORF57 protein binding.

In the case of EBV SM, very little specific binding to RNA targets has been demonstrable. An arginine-rich region of 33 amino acids has been identified as an RNA binding region in SM (17). This region does not strongly resemble classic RNA binding protein motifs, such as RGG boxes, KH domains, or RRM motifs. However, it contains two RS dipeptides and three other arginine residues. In vitro, no target-specific binding could be demonstrated using a peptide containing this motif (17). Limited comparisons of the affinity of SM for heterologous reporter gene RNAs suggested that SM bound equally well to luciferase and chloramphenicol acetyltransferase despite having markedly greater effects on chloramphenicol acetyltransferase RNA accumulation (33). Attempts to demonstrate site-specific RNA binding by in vitro cross-linking of SM to RNA revealed some preferential binding, but an ability to bind all the RNAs tested to some degree was observed (46). Gene-specific activation of expression despite apparently nonselective RNA binding by SM has been explained as possibly due to inherent differences in target transcripts (17, 33). For example, SM might bind nonspecifically to all RNAs but only affect the expression of those RNAs that are unstable or incapable of independent nuclear export. Alternatively, SM might act in a manner similar to that of cellular RNA binding proteins that have broad RNA binding properties yet achieve extremely specific effects on target RNAs. SR proteins that bind to short, degenerate sequences and hnRNPs, which have both nonspecific and specific RNA binding properties, are classic examples of such RNA binding proteins that exert gene-specific effects on alternative splicing. Such specific effects are achieved by combinatorial effects, context-dependent binding, and protein-protein interactions (40).

It is in this context that we investigated whether SM exhibits any preferential association with EBV RNAs during the course of lytic replication. In the current study, we chose to analyze SM-RNA interactions without UV cross-linking, under relatively gentle isolation conditions, in an attempt to preserve physiologic interactions. Overall, it is clear that there are large differences in the affinities of various RNAs for SM despite the fact that under the conditions used in these experiments, SM associated with the majority of EBV mRNAs.

While the abundance of an RNA species would be expected to affect the percentage found complexed with SM if RNA binding activity were nonspecific, it is clear that the extent to

which an RNA is associated with SM is not simply dependent on its abundance. It is likely, however, that the timing of the experiment, which was chosen to maximize the number of lytic RNAs that might be detected, affected the representation of RNAs that were detected in association with SM. These data therefore indicate that while SM does associate with a large number of RNAs in vivo, a hierarchy of affinities for SM exists among the various RNAs. Thus, it is unlikely that SM binds to or affects only RNAs that contain a critical response element, in the manner of human immunodeficiency virus Rev.

One caveat in our experiment is that the qRT-PCR primers were directed against individual ORFs. Hence, we do not know how ORF length, 3′ or 5′ UTR length, or the presence of multiple SM binding regions affect our quantitation. We therefore used ranking-based statistics (44) to identify ORFs that are encoded by mRNAs of as yet unspecified size that were bound by SM.

The finding that two of the most highly SM-associated RNAs in both P3HR1 and B95-8 cells exhibit region-specific binding to SM in vitro and in vivo suggests that binding of at least some RNAs to SM may be highly sequence or structure specific. Significantly, SM binding to these regions was correlated with the ability to enhance expression, suggesting that the specificity of SM action is mediated at least in part by binding specificity. Preferential binding to the 5′ and 3′ UTRs, albeit of only two transcripts, is similar to the behavior of other RNA regulatory proteins, such as eIF4E, which bind to so-called USER codes in the 5′ and 3′ UTRs of target mRNAs (10–12). Such USER codes consist of long, highly structured sequences, as well as relatively short (40-nt) sequences in the case of eIF4E. It is tempting to speculate that SM and its herpesvirus homologs may perform coordinate regulation of transcripts as an RNA regulon, as proposed by Keene and Tenenbaum (20). In this model, multiple transcripts may be regulated as a posttranscriptional operon, allowing a protein that binds to common elements in the UTRs of target genes to perform coordinated functions, such as nuclear export, on all such target mRNAs. The utility of an RNA regulon in herpesvirus replication is apparent when one considers the multitude of lytic transcripts that must be stabilized, exported, and translated in an efficient manner in a limited time. Whether one or more specific SM response elements are present in EBV transcripts, and possibly cellular transcripts, remains to be experimentally confirmed. There is no obvious homology between the 5′ UTRs of BFRF3 and BDLF3, nor is there an obvious bias in the nucleotide compositions of these regions. Further mapping of SM binding by in vitro cross-linking experiments such as the ones described here may allow the definition of one or more minimal binding sites. However, by analogy to SR proteins, which bind to degenerate consensus sequences and exhibit both general and specific RNA binding, definition of SM target specificity by bioinformatics analysis alone is unlikely to be successful, and further biochemical characterization of SM RNA interactions and definition of the crystal structure of SM and its homologs may be required (16). The identification of transcripts that are highly associated with SM in vivo should allow further characterization of specific elements involved in coordinate posttranscriptional regulation by SM.

ACKNOWLEDGMENTS

This work was supported by grants RO1 CA81133 (S.S.) and DE018304 (D.P.D.) from the National Institutes of Health and grant 6021-06 from the Leukemia and Lymphoma Society (D.P.D.).

We thank Rolf Renne and David Bloom for suggestions and reviews of our work.

REFERENCES

1. **Batisse, J., E. Manet, J. Middeldorp, A. Sergeant, and H. Gruffat.** 2005. Epstein-Barr virus mRNA export factor EB2 is essential for intranuclear capsid assembly and production of gp350. J. Virol. **79:**14102–14111.
2. **Bello, L. J., A. J. Davison, M. A. Glenn, A. Whitehouse, N. Rethmeier, T. F. Schulz, and J. Barklie Clements.** 1999. The human herpesvirus-8 ORF 57 gene and its properties. J. Gen. Virol. **80:**3207–3215.
3. **Boyle, S. M., V. Ruvolo, A. K. Gupta, and S. Swaminathan.** 1999. Association with the cellular export receptor CRM 1 mediates function and intracellular localization of Epstein-Barr virus SM protein, a regulator of gene expression. J. Virol. **73:**6872–6881.
4. **Brown, C. R., M. S. Nakamura, J. D. Mosca, G. S. Hayward, S. E. Straus, and L. P. Perera.** 1995. Herpes simplex virus *trans*-regulatory protein ICP27 stabilizes and binds to 3′ ends of labile mRNA. J. Virol. **69:**7187–7195.
5. **Buisson, M., F. Hans, I. Kusters, N. Duran, and A. Sergeant.** 1999. The C-terminal region but not the Arg-X-Pro repeat of Epstein-Barr virus protein EB2 is required for its effect on RNA splicing and transport. J. Virol. **73:**4090–4100.
6. **Buisson, M., E. Manet, M. C. Trescol-Biemont, H. Gruffat, B. Durand, and A. Sergeant.** 1989. The Epstein-Barr Virus (EBV) early protein EB2 is a posttranscriptional activator expressed under the control of EBV transcription factors EB1 and R. J. Virol. **63:**5276–5284.
7. **Chen, L., G. Liao, M. Fujimuro, O. J. Semmes, and S. D. Hayward.** 2001. Properties of two EBV Mta nuclear export signal sequences. Virology **288:** 119–128.
8. **Chevalier-Greco, A., E. Manet, P. Chavrier, C. Mosnier, J. Daillie, and A. Sergeant.** 1986. Both Epstein-Barr virus (EBV)-encoded *trans*-acting factors, EB1 and EB2, are required to activate transcription from an EBV early promoter. EMBO J. **5:**3243–3249.
9. **Colgan, K. J., J. R. Boyne, and A. Whitehouse.** 2009. Identification of a response element in a herpesvirus saimiri mRNA recognized by the ORF57 protein. J. Gen. Virol. **90:**596–601.
10. **Culjkovic, B., I. Topisirovic, and K. L. Borden.** 2007. Controlling gene expression through RNA regulons: the role of the eukaryotic translation initiation factor eIF4E. Cell Cycle **6:**65–69.
11. **Culjkovic, B., I. Topisirovic, L. Skrabanek, M. Ruiz-Gutierrez, and K. L. Borden.** 2006. eIF4E is a central node of an RNA regulon that governs cellular proliferation. J. Cell Biol. **175:**415–426.
12. **Culjkovic, B., I. Topisirovic, L. Skrabanek, M. Ruiz-Gutierrez, and K. L. Borden.** 2005. eIF4E promotes nuclear export of cyclin D1 mRNAs via an element in the 3′UTR. J. Cell Biol. **169:**245–256.
13. **Gluzman, Y.** 1981. SV40-transformed simian cells support the replication of early SV40 mutants. Cell **23:**175–182.
14. **Gruffat, H., J. Batisse, D. Pich, B. Neuhierl, E. Manet, W. Hammerschmidt, and A. Sergeant.** 2002. Epstein-Barr virus mRNA export factor EB2 is essential for production of infectious virus. J. Virol. **76:**9635–9644.
15. **Han, Z., E. Marendy, Y. D. Wang, J. Yuan, J. T. Sample, and S. Swaminathan.** 2007. Multiple roles of Epstein-Barr virus SM protein in lytic replication. J. Virol. **81:**4058–4069.
16. **Hargous, Y., G. M. Hautbergue, A. M. Tintaru, L. Skrisovska, A. P. Golovanov, J. Stevenin, L. Y. Lian, S. A. Wilson, and F. H. Allain.** 2006. Molecular basis of RNA recognition and TAP binding by the SR proteins SRp20 and 9G8. EMBO J. **25:**5126–5137.
17. **Hiriart, E., L. Bardouillet, E. Manet, H. Gruffat, F. Penin, R. Montserret, G. Farjot, and A. Sergeant.** 2003. A region of the Epstein-Barr virus (EBV) mRNA export factor EB2 containing an arginine-rich motif mediates direct binding to RNA. J. Biol. Chem. **278:**37790–37798.
18. **Hiriart, E., G. Farjot, H. Gruffat, M. V. Nguyen, A. Sergeant, and E. Manet.** 2003. A novel nuclear export signal and a REF interaction domain both promote mRNA export by the Epstein-Barr virus EB2 protein. J. Biol. Chem. **278:**335–342.
19. **Johannsen, E., M. Luftig, M. R. Chase, S. Weicksel, E. Cahir-McFarland, D. Illanes, D. Sarracino, and E. Kieff.** 2004. Proteins of purified Epstein-Barr virus. Proc. Natl. Acad. Sci. USA **101:**16286–16291.
20. **Keene, J. D., and S. A. Tenenbaum.** 2002. Eukaryotic mRNPs may represent posttranscriptional operons. Mol. Cell **9:**1161–1167.
21. **Kenney, S., J. Kamine, E. Holley-Guthrie, E. C. Mar, J. C. Lin, D. Markovitz, and J. Pagano.** 1989. The Epstein-Barr virus immediate-early gene product, BMLF1, acts in *trans* by a posttranscriptional mechanism which is reporter gene dependent. J. Virol. **63:**3870–3877.
22. **Kim, V. N., J. Yong, N. Kataoka, L. Abel, M. D. Diem, and G. Dreyfuss.** 2001. The Y14 protein communicates to the cytoplasm the position of exon-exon junctions. EMBO J. **20:**2062–2068.

23. **Kurokawa, M., S. K. Ghosh, J. C. Ramos, A. M. Mian, N. L. Toomey, L. Cabral, D. Whitby, G. N. Barber, D. P. Dittmer, and W. J. Harrington, Jr.** 2005. Azidothymidine inhibits NF-κB and induces Epstein-Barr virus gene expression in Burkitt lymphoma. Blood **106:**235–240.
24. **McCarthy, A. M., L. McMahan, and P. A. Schaffer.** 1989. Herpes simplex virus type 1 ICP27 deletion mutants exhibit altered patterns of transcription and are DNA deficient. J. Virol. **63:**18–27.
25. **Mears, E., and S. A. Rice.** 1996. The RGG box motif of the herpes simplex virus ICP27 protein mediates an RNA-binding activity and determines in vivo methylation. J. Virol. **70:**7445–7453.
26. **Miller, G., and M. Lipman.** 1973. Release of infectious Epstein-Barr virus by transformed marmoset leukocytes. Proc. Natl. Acad. Sci. USA **70:**190–194.
27. **Moriuchi, H., M. Moriuchi, H. A. Smith, and J. I. Cohen.** 1994. Varicella-zoster virus open reading frame 4 protein is functionally distinct from and does not complement its herpes simplex virus type 1 homolog, ICP27. J. Virol. **68:**1987–1992.
28. **Nicewonger, J., G. Suck, D. Bloch, and S. Swaminathan.** 2004. Epstein-Barr virus (EBV) SM protein induces and recruits cellular Sp110b to stabilize mRNAs and enhance EBV lytic gene expression. J. Virol. **78:**9412–9422.
29. **Papin, J., W. Vahrson, R. Hines-Boykin, and D. P. Dittmer.** 2005. Real-time quantitative PCR analysis of viral transcription. Methods Mol. Biol. **292:**449–480.
30. **Perera, L. P., S. Kaushal, P. R. Kinchington, J. D. Mosca, G. S. Hayward, and S. E. Straus.** 1994. Varicella-zoster virus open reading frame 4 encodes a transcriptional activator that is functionally distinct from that of herpes simplex virus homolog ICP27. J. Virol. **68:**2468–2477.
31. **Rabson, M., L. Gradoville, L. Heston, and G. Miller.** 1982. Non-immortalizing P3J-HR1 Epstein-Barr virus: a deletion mutant of its transforming parent, Jijoye. J. Virol. **48:**834–844.
32. **Reed, R., and H. Cheng.** 2005. TREX, SR proteins and export of mRNA. Curr. Opin. Cell Biol. **17:**269–273.
33. **Ruvolo, V., A. K. Gupta, and S. Swaminathan.** 2001. Epstein-Barr virus SM protein interacts with mRNA in vivo and mediates a gene-specific increase in cytoplasmic mRNA. J. Virol. **75:**6033–6041.
34. **Ruvolo, V., L. Sun, K. Howard, S. Sung, H. J. Delecluse, W. Hammerschmidt, and S. Swaminathan.** 2004. Functional analysis of Epstein-Barr virus SM protein: identification of amino acids essential for structure, transactivation, splicing inhibition, and virion production. J. Virol. **78:**340–352.
35. **Ruvolo, V., E. Wang, S. Boyle, and S. Swaminathan.** 1998. The Epstein-Barr virus nuclear protein SM is both a post-transcriptional inhibitor and activator of gene expression. Proc. Natl. Acad. Sci. USA **95:**8852–8857.
36. **Sacks, W. R., C. C. Greene, D. P. Aschman, and P. A. Schaffer.** 1985. Herpes simplex virus type 1 ICP27 is an essential regulatory protein. J. Virol. **55:**796–805.
37. **Sandri-Goldin, R. M.** 1998. ICP27 mediates HSV RNA export by shuttling through a leucine-rich nuclear export signal and binding viral intronless RNAs through an RGG motif. Genes Dev. **12:**868–879.
38. **Sandri-Goldin, R. M.** 2004. Viral regulation of mRNA export. J. Virol. **78:**4389–4396.
39. **Semmes, O. J., L. Chen, R. T. Sarisky, Z. Gao, L. Zhong, and S. D. Hayward.** 1998. Mta has properties of an RNA export protein and increases cytoplasmic accumulation of Epstein-Barr virus replication gene mRNA. J. Virol. **72:**9526–9534.
40. **Singh, R., and J. Valcarcel.** 2005. Building specificity with nonspecific RNA-binding proteins. Nat. Struct. Mol. Biol. **12:**645–653.
41. **Sokolowski, M., J. E. Scott, R. P. Heaney, A. H. Patel, and J. B. Clements.** 2003. Identification of herpes simplex virus RNAs that interact specifically with regulatory protein ICP27 in vivo. J. Biol. Chem. **278:**33540–33549.
42. **Swaminathan, S.** 2005. Post-transcriptional gene regulation by EBV SM protein, p. 631–650. *In* E. Robertson (ed.), Epstein-Barr virus. Caister Academic Press, Norfolk, United Kingdom.
43. **Toth, Z., P. Lischka, and T. Stamminger.** 2006. RNA-binding of the human cytomegalovirus transactivator protein UL69, mediated by arginine-rich motifs, is not required for nuclear export of unspliced RNA. Nucleic Acids Res. **34:**1237–1249.
44. **Troyanskaya, O. G., M. E. Garber, P. O. Brown, D. Botstein, and R. B. Altman.** 2002. Nonparametric methods for identifying differentially expressed genes in microarray data. Bioinformatics **18:**1454–1461.
45. **Verma, D., C. Ling, E. Johannsen, T. Nagaraja, and S. Swaminathan.** 2009. Negative autoregulation of Epstein-Barr virus (EBV) replicative gene expression by EBV SM protein. J. Virol. **83:**8041–8050.
46. **Verma, D., and S. Swaminathan.** 2008. Epstein-Barr virus SM protein functions as an alternative splicing factor. J. Virol. **82:**7180–7188.
47. **Winkler, M., S. A. Rice, and T. Stamminger.** 1994. UL69 of human cytomegalovirus, an open reading frame with homology to ICP27 of herpes simplex virus, encodes a transactivator of gene expression. J. Virol. **68:**3943–3954.
48. **Zhou, Z., M. J. Luo, K. Straesser, J. Katahira, E. Hurt, and R. Reed.** 2000. The protein Aly links pre-messenger-RNA splicing to nuclear export in metazoans. Nature **407:**401–405.